doi:10.1006/jmbi.2000.3639 available online at http://www.idealibrary.com on IDEAL® J. Mol. Biol. (2000) 298, 95–110

JMB

Aminoglycoside Binding in the Major Groove of Duplex RNA: The Thermodynamic and Electrostatic Forces that Govern Recognition

Emily Jin[1], Vsevolod Katritch[2], Wilma K. Olson[2,3], Malkhaz Kharatisvili[2] Ruben Abagyan[4] and Daniel S. Pilch[1,3]*

[1]*Department of Pharmacology University of Medicine and Dentistry of New Jersey-Robert Wood Johnson Medical School 675 Hoes Lane, Piscataway NJ 08854, USA*

[2]*Department of Chemistry Rutgers-The State University of New Jersey, Piscataway NJ 08854, USA*

[3]*The Cancer Institute of New Jersey, New Brunswick NJ 08901, USA*

[4]*New York University Medical Center, Skirball Institute, New York, NY 10016, USA*

**Corresponding author*

We use a combination of spectroscopic, calorimetric, viscometric and computer modeling techniques to characterize the binding of the aminoglycoside antibiotic, tobramycin, to the polymeric RNA duplex, poly(rI)·poly(rC), which exhibits the characteristic *A*-type conformation that is conserved among natural and synthetic double-helical RNA sequences. Our results reveal the following significant features: (i) CD-detected binding of tobramycin to poly(rI)·poly(rC) reveals an apparent site size of four base-pairs per bound drug molecule; (ii) tobramycin binding enhances the thermal stability of the host poly(rI)·poly(rC) duplex, the extent of which decreases upon increasing in Na^+ concentration and/or pH conditions; (iii) the enthalpy of tobramycin-poly(rI)·poly(rC) complexation increases with increasing pH conditions, an observation consistent with binding-induced protonation of one or more drug amino groups; (iv) the affinity of tobramycin for poly(rI)·poly(rC) is sensitive to both pH and Na^+ concentration, with increases in pH and/or Na^+ concentration resulting in a concomitant reduction in binding affinity. The salt dependence of the tobramycin binding affinity reveals that the drug binds to the host RNA duplex as trication. (v) The thermodynamic driving force for tobramycin-poly(rI)·poly(rC) complexation depends on pH conditions. Specifically, at pH $\leqslant$ 6.0, tobramycin binding is entropy driven, but is enthalpy driven at pH > 6.0. (vi) Viscometric data reveal non-intercalative binding properties when tobramycin complexes with poly(rI)·poly(rC), consistent with a major groove-directed mode of binding. These data also are consistent with a binding-induced reduction in the apparent molecular length of the host RNA duplex. (vii) Computer modeling studies reveal a tobramycin-poly(rI)·poly(rC) complex in which the drug fits snugly at the base of the RNA major groove and is stabilized, at least in part, by an array of hydrogen bonding interactions with both base and backbone atoms of the host RNA. These studies also demonstrate an inability of tobramycin to form a stable low-energy complex with the minor groove of the poly(rI)·poly(rC) duplex. In the aggregate, our results suggest that tobramycin-RNA recognition is dictated and controlled by a broad range of factors that include electrostatic interactions, hydrogen bonding interactions, drug protonation reactions, and binding-induced alterations in the structure of the host RNA. These modulatory effects on tobramycin-RNA complexation are discussed in terms of their potential importance for the selective recognition of specific RNA structural motifs, such as asymmetric internal loops or hairpin loop-stem junctions, by aminoglycoside antibiotics and their derivatives.

Present address: V. Katritch and R. Abagyan, The Scripps Research Institute, Department of Molecular Biology, 10550 North Torrey Pines Road, La Jolla, CA 92037, USA.

Abbreviations used: p(rI)·p(rC), poly(rI)·poly(rC); r_{bp}, ratio of total drug to base-pairs; T_m, melting temperature; ITC, isothermal titration calorimetry; DSC, differential scanning calorimetry; CD, circular dichroism.

E-mail address of the corresponding author: pilch@rutchem.rutgers.edu

0022-2836/00/010095–16 $35.00/0

Keywords: aminoglycoside-RNA recognition; binding-induced drug protonation; drug-induced alteration in RNA structure; RNA bending and hydration; isothermal titration calorimetry

Introduction

RNA is a versatile molecule capable of folding into a broad range of different structures and/or conformations. These structures can serve as specific drug recognition elements. The targeting of drugs to specific RNA structures and/or sequences offers the possibility of modulating the biological activities of the host RNA molecules (Ecker & Griffey, 1999; Tor, 1999; Schroeder *et al*., 2000). A number of different classes of RNA-binding drugs have been identified to date (reviewed by Chow & Bogdan, 1997; Wallis & Schroeder, 1997; Michael & Tor, 1998). These structurally and chemically diverse families of drugs include the aminoglycoside antibiotics (e.g. neomycin B and tobramycin) (Schroeder & von Ahsen, 1996; Michael & Tor, 1998; Tor, 1999; Schroeder *et al*., 2000), cyclic peptides (e.g. viomycin and thiostrepton) (Ryan & Draper, 1991; Wallis *et al*., 1997), heterocyclic intercalating compounds (e.g. ethidium bromide) (Waring, 1966; Douthart *et al*., 1973; Nelson & Tinoco, 1984), and various aromatic diamidines (e.g. berenil and pentamidine) (Liu *et al*., 1994; Pilch *et al*., 1995b).

Many of the known RNA-directed drugs exert their biological/therapeutic influence by binding to the ribosomal RNA (rRNA) and interfering with translation (Vázquez, 1979; Spahn & Prescott, 1996; Wallis & Schroeder, 1997; Tor, 1999). In recent years, three new classes of RNA molecules have been have been identified as drug targets (Schroeder & von Ahsen, 1996; Tor, 1999; Schroeder *et al*., 2000). The first class is comprised of catalytic RNA molecules or ribozymes, which include the self-splicing group I introns (von Ahsen *et al*., 1991; von Ahsen & Noller, 1993; Liu *et al*., 1994) and the hammerhead ribozyme (Clouet-d'Orval *et al*., 1995; Stage *et al*., 1995; Wang & Tor, 1997, 1998; Hermann & Westhof, 1998). The second class of RNA targets contains protein binding sites, and includes the Rev responsive element (RRE) of HIV (Zapp *et al*., 1993, 1997; Werstuck *et al*., 1996; Hendrix *et al*., 1997) as well as the *trans*-activating region (TAR) of HIV (Hamy *et al*., 1998; Mei *et al*., 1998; Wang *et al*., 1998). The third class of target sites contains sequences (aptamers) that have been selected *in vitro* for specific and high-affinity drug binding (Wang & Rando, 1995; Wang *et al*., 1996; Jiang *et al*., 1997; Patel *et al*., 1997; Hamasaki *et al*., 1998; Jiang & Patel, 1998).

The aminoglycoside antibiotics represent a family of drugs that are used primarily in the treatment of infections caused by aerobic Gram-negative bacteria (Chambers & Sande, 1996). They consist of one or more amino sugars joined to a six-carbon aminocyclitol moiety *via* glycosidic linkages (Chambers & Sande, 1996). The aminoglycoside molecules exert their bactericidal activity by binding directly to the 16 S rRNA in the 30 S subunit of the ribosome and interfering with the translocation step of the translation process (Schroeder & von Ahsen, 1996; Schroeder *et al*., 2000, and references therein). Aminoglycoside binding also can modulate the functional and/or catalytic activities of other RNA molecules, including various group I introns (von Ahsen *et al*., 1991; von Ahsen & Noller, 1993; Liu *et al*., 1994; Waldsich *et al*., 1998), the RRE of HIV (Zapp *et al*., 1993; Werstuck *et al*., 1996), and the TAR of HIV (Mei *et al*., 1998; Wang *et al*., 1998). Thus, aminoglycosides are potentially useful both as antimicrobial and as antiviral agents.

Chemical and enzymatic footprinting analyses have been used to define the sites of aminoglycoside interaction on a broad range of microbial and viral RNA molecules (von Ahsen & Noller, 1993; Zapp *et al*., 1993; Recht *et al*., 1996; Fourmy *et al*., 1998a; Mei *et al*., 1998; Kirk & Tor, 1999). In addition, *in vitro* selection techniques have yielded a number of different RNA sequences that bind aminoglycosides with a high degree of specificity (Lato *et al*., 1995; Wallis *et al*., 1995; Wang & Rando, 1995; Wang *et al*., 1996; Hamasaki *et al*., 1998; Werstuck & Green, 1998). In the aggregate, these studies have revealed a pattern suggesting that RNA regions containing either asymmetric internal loops or hairpin loop-stem junctions are preferential binding sites for aminoglycosides. These RNA binding preferences are consistent with those reported in recent NMR studies by both the Puglisi (Fourmy *et al*., 1996; Recht *et al*., 1996; Fourmy *et al*., 1998a,b) and Patel (Jiang *et al*., 1997; Jiang & Patel, 1998) groups on different aminoglycoside-RNA complexes. Puglisi and co-workers found that neomycin-class aminoglycosides preferentially bind to an asymmetric internal loop of an RNA oligomer modeling the A-site of the *Escherichia coli* 16 S rRNA (Fourmy *et al*., 1996, 1998a,b; Recht *et al*., 1996). Patel and co-workers described the solution structure of a tobramycin-RNA aptamer complex in which the drug was centered about a hairpin loop-stem junction site (Jiang *et al*., 1997; Jiang & Patel, 1998). Significantly, both sets of NMR studies were consistent in demonstrating that the binding of the aminoglycosides is directed to the major groove of the host RNA duplex. These NMR studies have provided evidence for the major groove-directed binding of aminoglycosides to RNA duplexes whose major grooves are distorted by the presence of a loop or bulge. In another elegant set of NMR studies, the Shafer and

Kuntz groups used ^{19}F solvent isotope shift (SIS) measurements to demonstrate that the binding of aminoglycosides to ''normal'' RNA duplexes is also directed to the major groove (Chen *et al.*, 1997).

In addition to *A*-form RNA duplexes, aminoglycosides also can bind to DNA duplexes, while facilitating or inducing the conversion from the *B* to the *A*-conformation (Robinson & Wang, 1996; Chen *et al.*, 1997). NMR studies by the Wang group have suggested that the aminoglycoside neomycin, as well as the oligovalent cationic ligands $Co(NH_3)_6^{3+}$ and spermine, share a common structural basis for inducing the *B* to *A*-DNA conversion, which involves interactions between the cationic ligands and bases in the floor of the major groove of the host duplex (Robinson & Wang, 1996). Taken together, these observations suggest that aminoglycosides are specific for *A*-form relative to *B*-form nucleic acid duplexes, with this conformational specificity being due, at least in part, to favorable interactions deep within the major groove of the host *A*-form duplex.

The footprinting and NMR studies noted above have provided information regarding the sequence/structural specificities of aminoglycosides. However, comparatively little is known about the thermodynamic properties that govern the nucleic acid binding events. This deficiency limits our understanding of the molecular forces that dictate and control the affinity and specificity of binding. Here, we use a combination of spectroscopic, calorimetric, viscometric and computer modeling techniques to characterize the binding of the aminoglycoside antibiotic, tobramycin (see the structure in Figure 1), to the polymeric RNA duplex, poly(rI)·poly(rC) (hereafter abbreviated as p(rI)·p(rC)), which exhibits the characteristic *A*-type conformation that is conserved among natural and synthetic double-helical RNA sequences (Saenger, 1983). Our results demonstrate that the binding of tobramycin to RNA is governed by a broad range of factors, including solution conditions (e.g. salt concentration and pH), electrostatic interactions, hydrogen bonding interactions, drug protonation reactions, and binding-induced alterations in the structure of the host RNA. We discuss how such properties may contribute to the preferential binding of aminoglycosides to specific RNA structural motifs, such as asymmetric internal loops or hairpin loop-stem junctions.

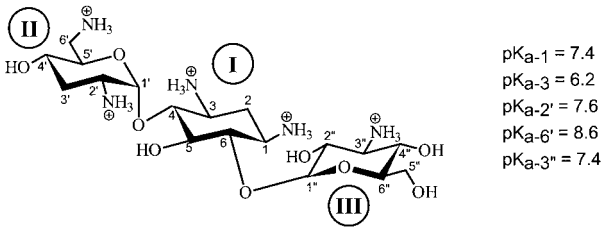

Figure 1. The structure of tobramycin in which the atomic and ring numbering systems are denoted in Arabic and Roman numerals, respectively. The NMR-derived (Dorman *et al.*, 1976; Koch *et al.*, 1978) pK_a values of the five amino groups are indicated.

Results and Discussion

CD-detected tobramycin binding to the p(rI)·p(rC) duplex reveals an apparent binding site size of four base-pairs

Figure 2(a) shows the CD spectra from 220 nm to 320 nm obtained by incremental titration of tobramycin into a solution of p(rI)·p(rC) at 60 mM Na^+ and pH 6.0. Note that addition of tobramycin alters the CD spectrum of the p(rI)·p(rC) duplex. These changes in duplex CD properties are indicative of interactions between tobramycin and p(rI)·p(rC), and can be used to detect and monitor tobramycin binding. Figure 2(b) shows the titration curve at 244 nm extracted from the family of CD spectra shown in Figure 2(a). In this curve, the data points represent the experimental molar ellipticities of the host RNA duplex, while the continuous lines reflect linear least-squares fits of each apparent linear domain of the experimental data points. Inspection of Figure 2(b) reveals a single apparent inflection point, an observation consistent with a single, CD-detectable tobramycin binding event when p(rI)·p(rC) serves as the host duplex. Note that this observed inflection point corresponds to a total tobramycin to base-pair ratio (r_{bp}) of 0.25. The reciprocal of this r_{bp} value provides an estimate for the apparent number of base-pairs influenced by tobramycin binding (i.e. the binding site size). In other words, tobramycin binding to p(rI)·p(rC) influences an apparent site size (n) of 4 bp per bound drug molecule.

As noted above, tobramycin binding alters the CD spectrum of p(rI)·p(rC) (see Figure 2(a)). These drug-induced alterations in duplex CD properties, which include a decrease in the intensity of the positive band at 244 nm and a concomitant increase in the intensity of the positive band at 278 nm, are consistent with a binding-induced change in the structure/conformation of the host p(rI)·p(rC) duplex. Note that these tobramycin-induced changes in the CD properties of p(rI)·p(rC) are similar, albeit smaller in magnitude, to those induced by the anticancer drug cisplatin (Hermann & Guschlbauer, 1978). Cisplatin is known to bind and cross-link nucleic acids, with the major adduct being an intrastrand cross-link between the N7 atoms of neighboring purine bases (Sherman & Lippard, 1987; Bruhn *et al.*, 1990). Furthermore, formation of the cisplatin intrastrand cross-link bends the host duplex in the direction of the major groove (Takahara *et al.*, 1995, 1996; Gelasco & Lippard, 1998). Hence, it is reasonable to suggest that the tobramycin-induced alterations in p(rI)·p(rC) CD properties observed here reflect a binding-induced bending of the host RNA duplex in the direction of the major groove. In fact, as dis-

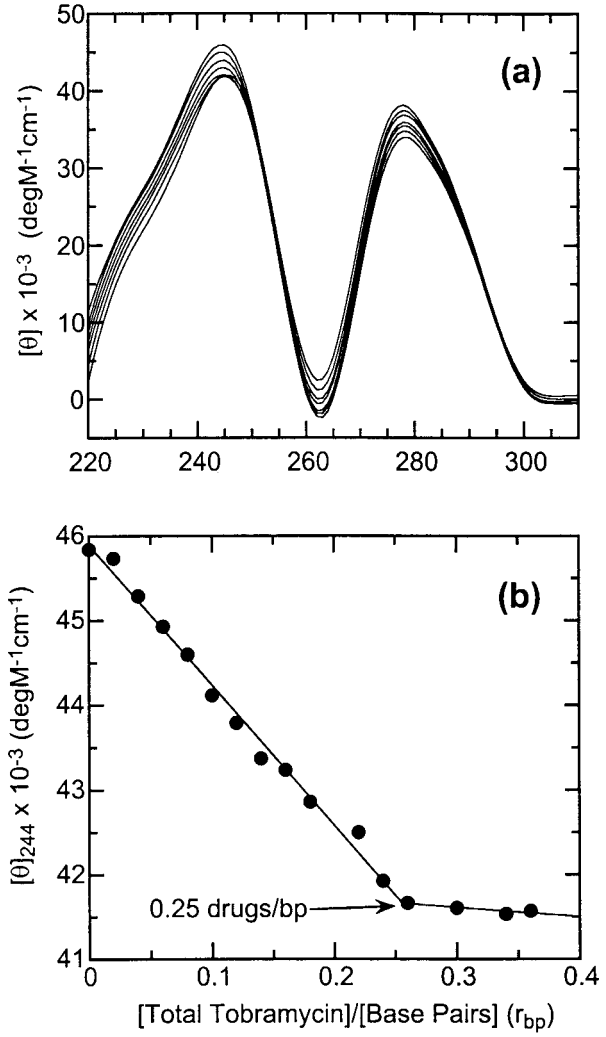

Figure 2. (a) CD titration of p(rI)·p(rC) (60 μM bp) with tobramycin at 25 °C in pH 6.0 buffer containing 10 mM sodium cacodylate (7 mM Na^+), 10 mM Mops (9.5 mM Na^+), 43.5 mM NaCl, and 0.1 mM EDTA. From top to bottom at 244 nm, the CD spectra correspond to drug/base-pair (r_{bp}) ratios of 0, 0.06, 0.12, 0.18, 0.24, 0.30, and 0.36. (b) Normalized molar ellipticity at 244 nm ($[\theta]_{244}$) as a function of the r_{bp} ratio. The continuous lines reflect the linear least-squares fits of each apparent linear domain of the experimental data (filled circles) before and after the apparent inflection point. The r_{bp} ratio (0.25) corresponding to the apparent inflection point is indicated. Molar ellipticity is per molar base-pair.

cussed below, our viscometric and computer modeling data are consistent with tobramycin-induced reductions in both the apparent molecular length and major groove width of the host p(rI)·p(rC) duplex. This type of binding-induced allosteric behavior has been observed recently by Puglisi and co-workers in NMR studies on the complexation of the aminoglycoside antibiotic, paromomycin, with an RNA oligomer that models the *A*-site of the *E. coli* 16 S rRNA (Fourmy *et al.*, 1996, 1998a,b).

Tobramycin binding enhances the thermal stability of the p(rI)·p(rC) duplex in a manner that is sensitive to both pH and Na^+ concentration

UV melting experiments were conducted in the absence and presence of tobramycin to assess the impact, if any, of the ligand on the thermal stability of p(rI)·p(rC). The resulting melting profiles are shown in Figure 3. Note that at pH 5.5 (at which tobramycin is essentially in its fully protonated state with a corresponding charge of +5) and a Na^+ concentration of 60 mM, the presence of tobramycin at an r_{bp} ratio of 0.25 increases the thermal stability (T_m) of the host duplex by 36.7 deg. C (Figure 3(a)). Higher r_{bp} ratios than 0.25 result in only marginal increases in the T_m of p(rI)·p(rC), an observation suggestive of some non-specific, secondary binding to the host duplex at high tobramycin concentrations. The tobramycin-induced enhancement in duplex thermal stability noted above is consistent with tobramycin binding to the host RNA duplex, with a preference for the double-stranded *versus* the single-stranded state (Crothers, 1971; McGhee, 1976). The extent of this thermal enhancement (ΔT_m) is sensitive to both pH and Na^+ concentration. Specifically, at a constant Na^+ concentration of 60 mM, raising the pH from 5.5 to 7.5 results in a decrease in ΔT_m from 36.7 to 8.0 °C (compare Figure 3(a) and (b)). Similarly, at a constant pH of 5.5, raising the Na^+ concentration from 60 to 350 mM results in a decrease in ΔT_m from 36.7 to 4.7 °C (compare Figure 3(a) and (c)). Thus, the extent to which tobramycin binding thermally stabilizes the host p(rI)·p(rC) duplex decreases with increasing pH and/or Na^+ concentration. This Na^+ and pH dependence of ΔT_m is consistent with at least one drug NH_3^+ group playing an important role in the binding of tobramycin to the host p(rI)·p(rC) duplex. In fact, as discussed below, the salt dependence of the tobramycin-p(rI)·p(rC) association constant is consistent with three drug NH_3^+ groups participating in electrostatic interactions with the host RNA duplex.

The observed enthalpy of tobramycin-p(rI)·p(rC) complexation becomes increasingly exothermic (favorable) with increasing pH

We used isothermal titration calorimetry (ITC) to determine the enthalpy of tobramycin-p(rI)·p(rC) complexation over a range of pH values. Figure 4 shows representative ITC profiles resulting from six sequential injections of tobramycin into a p(rI)·p(rC) solution at a constant Na^+ concentration of 60 mM and a pH value of either 5.5, 6.0, or 7.0. Each of the heat burst curves in Figure 4 correspond to a single tobramycin injection, with the six injections resulting in a final r_{bp} ratio of 0.09. The areas under these heat burst curves, as well as those for tobramycin-p(rI)·p(rC) complexation at pH values of 6.5, 7.5, and 8.0 (not shown),

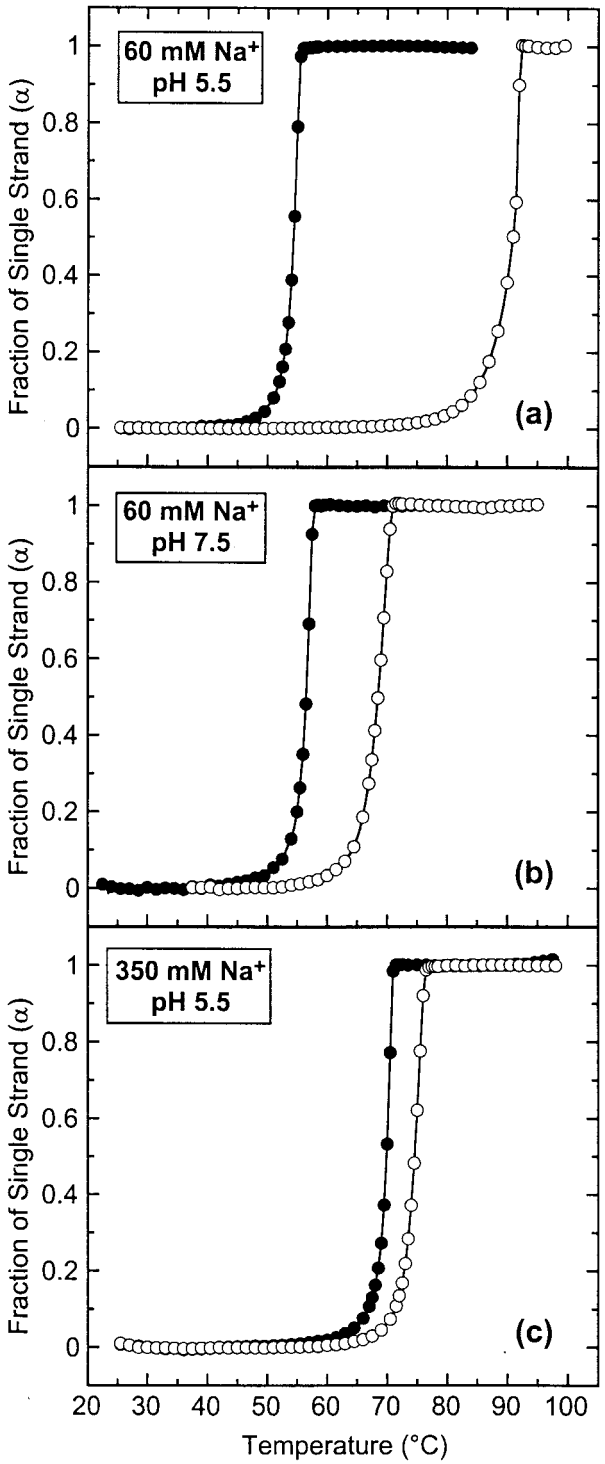

Figure 3. UV melting profiles for the p(rI)·p(rC) duplex (filled circles) and its tobramycin complex (open circles) at a drug to base-pair ratio (r_{bp}) of 0.25. The Na^+ concentrations and pH values are as indicated. For clarity of presentation, the melting curves were normalized by subtraction of the upper and lower baselines to yield plots of fraction single strand (α) *versus* temperature (Marky & Breslauer, 1987). All the UV melting profiles were acquired at 246 nm.

were determined by integration to yield the associated injection heats. Note that at each pH value, the six injection heats were similar in magnitude, an observation consistent with all the injected tobramycin being bound by the host RNA. These injection heats were corrected by subtraction of the corresponding dilution heats derived from the injection of identical amounts of tobramycin into buffer alone. The resulting corrected injection heats then were divided by the total concentration of injected tobramycin and averaged to yield the tobramycin binding enthalpies (ΔH_b) listed in Table 1.

Inspection of the data in Table 1 reveals a ΔH_b of −2.2 kcal/mol at pH 5.5. Note that tobramycin is essentially 100 % protonated at this pH (Dorman *et al.*, 1976; Koch *et al.*, 1978). Thus, our observed binding enthalpy at pH 5.5 (−2.2 kcal/mol) reflects the intrinsic heat associated with the binding of the pentacationic form of tobramycin to the host p(rI)·p(rC) duplex. Further note that as the pH value increases above 5.5, thereby reducing the extent of tobramycin protonation (see Figure 1 for the pK_a values of tobramycin), ΔH_b becomes increasingly negative (exothermic), ranging from −2.2 kcal/mol at pH 5.5 to −13.8 kcal/mol at pH 8.0. In other words, the enthalpy of tobramycin-p(rI)·p(rC) complexation becomes increasingly favorable with increasing pH. This observation can be explained if one considers that the protonation of an NH_2 group is a known exothermic reaction. For example, protonation of the 2-NH_2 group on D-glucosamine is accompanied by an enthalpy change of −5.3 kcal/mol (Miyamoto & Kazuko, 1958), while the protonation of amino acid α-NH_2 groups is accompanied by an average enthalpy change of approximately −10.0 kcal/mol (Tinoco *et al.*, 1978). Recall that our pH and salt-dependent ΔT_m data were consistent with at least one drug NH_3^+ group participating in interactions with the host RNA duplex. Thus, it is likely that the pH dependence of the tobramycin-p(rI)·p(rC) binding enthalpy noted above reflects exothermic contributions from binding-induced protonation of one or more drug NH_2 groups. In this connection, our pH-dependent tobramycin-p(rI)·p(rC) binding affinity data discussed below are consistent with RNA

Table 1. pH dependence of the calorimetrically determined enthalpy of tobramycin-p(rI)·p(rC) complexation at a constant Na^+ concentration of 60 mM

pH	ΔH_b [a] (kcal/mol)
5.5	−2.2 ± 0.2
6.0	−4.7 ± 0.2
6.5	−6.8 ± 0.1
7.0	−8.2 ± 0.1
7.5	−10.5 ± 0.1
8.0	−13.8 ± 0.1

[a] Binding enthalpies (ΔH_b) were determined by ITC as described in the text.

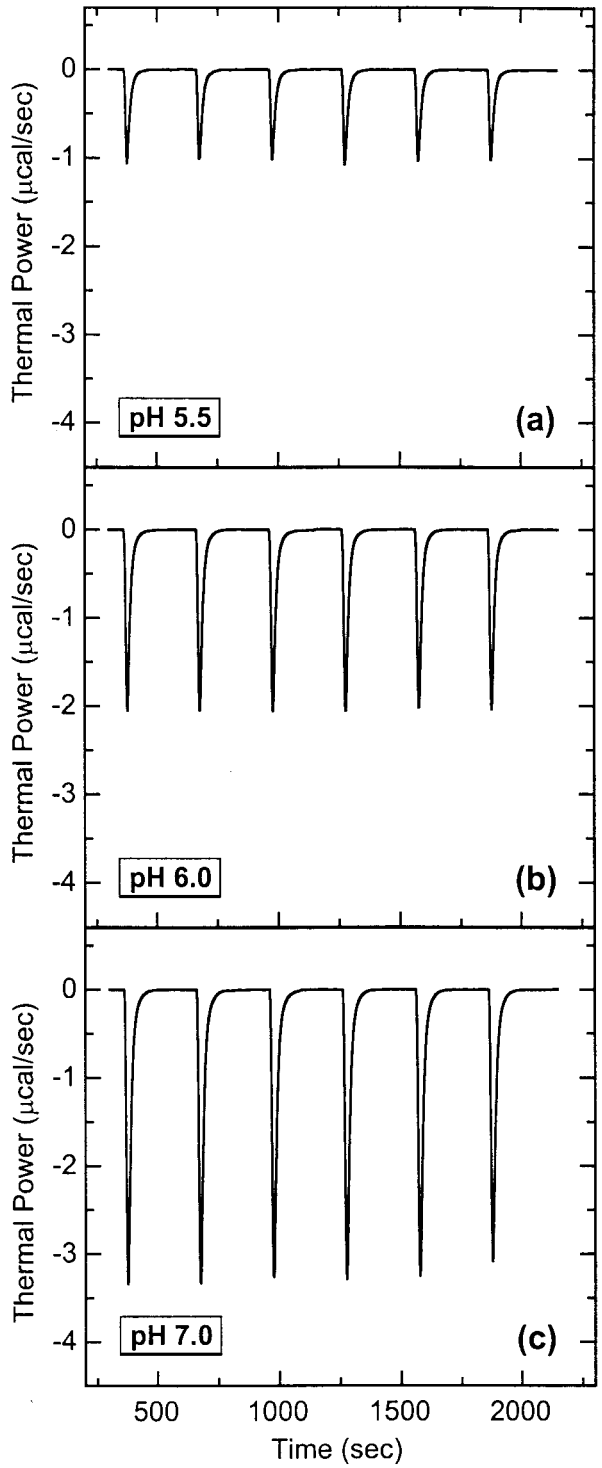

Figure 4. ITC profiles at 25 °C for the titration of tobramycin into a 500 μM bp solution of p(rI)·p(rC) at (a) pH 5.5, (b) 6.0, or (c) 7.0. Each heat burst curve is the result of a 5 μl injection of 2 mM tobramycin, with all six injections resulting in a final drug to base-pair ratio (r_{bp}) of 0.09. For all the ITC measurements, the buffer contained 60 mM Na^+.

binding at pH values >5.5 being coupled to protonation of the drug.

The pH dependence of tobramycin binding affinity for p(rI)·p(rC) is consistent with binding-induced protonation of one or more drug amino groups

We used the ΔT_m method described below to derive tobramycin-p(rI)·p(rC) association constants over a range of pH values. Measured tobramycin-induced changes in the thermal stability of p(rI)·p(rC) (see Figure 3) were used in conjunction with the 4 bp binding site size (n) derived from our CD measurements (see Figure 2) to estimate the apparent tobramycin-p(rI)·p(rC) association constants at T_m (K_{T_m}) from the following expression (Crothers, 1971):

$$\frac{1}{T_{m0}} - \frac{1}{T_m} = \frac{R}{n(\Delta H_{WC})} \ln(1 + K_{T_m} L) \qquad (1)$$

In this expression, T_{m0} and T_m are the melting temperatures of the drug-free and drug-saturated duplex, respectively, ΔH_{WC} is the enthalpy change for the melting of a Watson-Crick (WC) base-pair in the absence of bound drug (a value we determined independently for p(rI)·p(rC) using differential scanning calorimetry (DSC)), and L is the free drug concentration at T_m (which can be estimated by one half the total drug concentration). We then used the binding enthalpies (ΔH_b) listed in Table 1 to extrapolate these calculated binding constants at T_m to a common reference temperature of 25 °C using the standard relationship:

$$\frac{\partial \ln K}{\partial (1/T)} = -\frac{\Delta H_b}{R} \qquad (2)$$

Table 2 summarizes the apparent association constants at 25 °C (K_{25}) that we have calculated using equations (1) and (2) for tobramycin binding to the p(rI)·p(rC) duplex over a range of pH values. Note that, as the pH is raised from 5.5 to 6.5, the ΔT_m decreases from 36.7 to 25.7 °C. Despite this decrease in ΔT_m, K_{25} remains essentially unchanged at 4.4-5.0 × 10^7 M^{-1}. In other words, over the pH range of 5.5 to 6.5, the magnitude of ΔT_m does not correlate with the strength of binding (i.e. the magnitude of K_{25}). Equations (1) and (2) indicate that the relationship between ΔT_m and K_{25} depends on the binding enthalpy (ΔH_b). Recall that ΔH_b becomes increasingly exothermic with increasing pH, ranging from −2.2 kcal/mol at pH 5.5 to −6.8 kcal/mol at pH 6.5 (Table 1). This pH dependence of ΔH_b gives rise to the lack of concordance between the changes in ΔT_m and K_{25} over the pH range of 5.5 to 6.5.

Further inspection of the data in Table 2 reveals that as the pH increases above 6.5, both ΔT_m and K_{25} decrease concomitantly. In other words, a pH-induced reduction in the extent of tobramycin protonation is accompanied by a concomitant reduction in the affinity of the drug for the p(rI)·p(rC) host duplex. This observation, coupled with the pH-dependent ΔH_b data shown in Table 1,

Table 2. pH dependence of ΔT_m-derived association constants at 25 °C for the complexation of tobramycin with the p(rI)·p(rC) duplex at a constant Na^+ concentration of 60 mM

pH	T_{m0} (°C)[a]	T_m (°C)[a]	K_{25} (M^{-1})[b]
5.5	54.3	91.0	$46(\pm7) \times 10^6$
6.0	55.7	87.5	$50(\pm7) \times 10^6$
6.5	56.5	82.2	$44(\pm6) \times 10^6$
7.0	56.8	75.5	$20(\pm3) \times 10^6$
7.5	56.5	68.5	$8.9(\pm1.3) \times 10^6$
8.0	56.3	60.1	$1.8(\pm0.3) \times 10^6$

[a] T_m values were derived from UV melting profiles of p(rI)·p(rC) in the absence (T_{m0}) and presence of tobramycin (at a total tobramycin to bp ratio (r_{bp}) of 0.25), with an uncertainty in the data of ±0.2 deg. C.

[b] Binding constants at 25 °C (K_{25}) were determined using equations (1) and (2) as described in the text. For application of equation (1), we used DSC to determine the requisite values of ΔH_{WC} (+8.1 kcal/mol bp over the pH range of $6.5 \leqslant pH \leqslant 8.0$ and +7.7 kcal/mol bp at pH values of 5.5 and 6.0). For application of equation (2), we used ITC to determine the requisite values of ΔH_b listed in Table 1.

suggests that at pH values (pH > 5.5) where tobramycin is not fully protonated, its binding to p(rI)·p(rC) is accompanied by protonation of one or more of its NH_2 groups. As discussed below, our salt-dependent binding data are consistent with tobramycin-p(rI)·p(rC) complexation involving electrostatic interactions between the host RNA and three protonated (charged) drug amino groups. Hence, it is reasonable to suggest that one or more of these three drug NH_2 groups becomes protonated upon tobramycin complexation with p(rI)·p(rC) at pH values greater than 5.5. Our computer modeling studies (discussed below) suggest that these three NH_2 groups may be located on rings I and II of the drug.

The salt dependence of the tobramycin binding affinity for p(rI)·p(rC) reveals that the drug binds to the host RNA as a trication

We used the ΔT_m method described above to derive tobramycin-p(rI)·p(rC) association constants at 25 °C over a range of Na^+ concentrations at a constant pH of either 5.5 or 7.0. The resulting K_{25} values are summarized in Table 3. Note that at either pH value, K_{25} decreases with increasing Na^+ concentration. This observation suggests that electrostatic interactions play an important role in the binding of tobramycin to the host RNA duplex. The apparent number of drug NH_3^+ groups that participate in electrostatic interactions with the host RNA can be estimated from plots of $\log(K_{25})$ *versus* $\log([Na^+])$. Such plots for the data listed in Table 3 are shown in Figure 5. The observed linear dependencies can be described by the following relationship (deHaseth *et al.*, 1977; Record *et al.*, 1978):

$$\log(K_{obsd}) = \log(K^\circ) - m\psi \log([Na^+]) \qquad (3)$$

In this relationship, K_{obsd} is the observed binding constant, m is the number of ion pairs formed between the drug and the host RNA (a value that provides an estimate for the apparent valence of the RNA-bound drug), ψ is the thermodynamic counterion binding parameter for the host RNA (defined in the footnote to Table 4), and K° is the equilibrium constant for the following molecular reaction:

$$\text{Drug} + \text{RNA} \overset{K^\circ}{\rightleftharpoons} \text{Drug-RNA} + m\psi Na^+$$

Use of equation (3) to analyze the $\log(K_{25})$ *versus* $\log([Na^+])$ plots shown in Figure 5 yields the $-m\psi$ (slope) and $\log(K^\circ)$ (y-intercept) values listed in Table 4. Note that the slopes ($-m\psi$ values) of the

Table 3. Salt dependence of the ΔT_m-derived association constants at 25 °C for the complexation of tobramycin with the p(rI)·p(rC) duplex at a constant pH of either 5.5 or 7.0

$[Na^+]$ (mM)	T_{mo} (°C)[a]	T_m (°C)[a]	K_{25} (M^{-1})[b]
A. *pH = 5.5*			
60	54.3	91.0	$456(\pm68) \times 10^5$
110	61.1	84.4	$73(\pm11) \times 10^5$
180	65.0	79.9	$21(\pm3) \times 10^5$
350	69.9	74.6	$2.8(\pm0.4) \times 10^5$
B. *pH = 7.0*			
35	52.0	80.3	$951(\pm143) \times 10^5$
60	56.8	75.5	$198(\pm30) \times 10^5$
110	61.4	71.6	$42(\pm6) \times 10^5$
180	65.2	69.4	$9.9(\pm1.5) \times 10^5$

[a] T_m values were derived from UV melting profiles of p(rI)·p(rC) in the absence (T_{mo}) and presence of tobramycin (at a total tobramycin to bp ratio (r_{bp}) of 0.25), with an uncertainty in the data of ±0.2 deg. C.

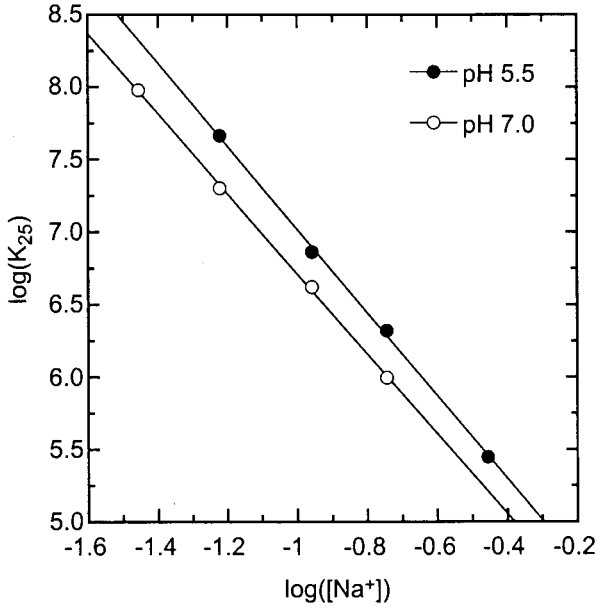

Figure 5. Salt dependence of the tobramycin binding affinity for p(rI)·p(rC). Log(K_{25}) *versus* log([Na^+]) plots for tobramycin complexation with the p(rI)·p(rC) duplex at pH 5.5 (filled circles) or 7.0 (open circles). These data were fit with equation (3) (continuous line) to yield the results summarized in Table 4.

log(K_{25}) *versus* log([Na^+]) plots at pH 5.5 and 7.0 are similar (−2.9 and −2.8, respectively). In conjunction with a ψ value of 0.89 for p(rI)·p(rC) (Record *et al.*, 1978), we calculate that at pH values of 5.5 and 7.0, p(rI)·p(rC)-bound tobramycin exhibits an apparent valence of +3.2 and +3.1, respectively. Thus, even under conditions (pH 5.5) where it exists in a pentacationic state, tobramycin binds to the host RNA as a trication. In other words, tobramycin-p(rI)·p(rC) complexation results in the formation of approximately three ion pairs between the drug and the host RNA, an observation consistent with only three out of a possible five drug NH_3^+ groups participating in electrostatic interactions with the host RNA.

Record and co-workers have shown that the non-specific binding of a trivalent cation to the p(rI)·p(rC) duplex is accompanied by a log(K°) value of 0.69 (Record *et al.*, 1976, 1978). The log(K°) values we determine for tobramycin binding to p(rI)·p(rC) (4.15 at pH 5.5 and 3.95 at pH 7.0) differ markedly from this prediction, suggesting that the complexation of each drug molecule is associated with large electrostatic contributions from specific interactions (e.g. hydrogen bonds and/or stereo-specific ion pairs) with its target site on the host RNA duplex. In previous studies, we observed a similar result for the binding of the dicationic, antitrypanosomal agent berenil to the poly(rA)·poly(rU) host duplex (Pilch *et al.*, 1995b).

Thermodynamic origins of the tobramycin binding affinity for the p(rI)·p(rC) duplex: drug binding at pH ⩽ 6.0 is entropy driven, while drug binding at pH>6.0 is enthalpy driven

Armed with the binding constants listed in Table 2, we calculated the corresponding binding free energies (ΔG_b) using the following standard relationship:

$$\Delta G_b = -RT \ln(K) \quad (4)$$

These binding free energies, coupled with our calorimetrically determined binding enthalpies listed in Table 1, allowed us to calculate the corresponding entropic contributions to binding ($T\Delta S_b$; where ΔS_b is the binding entropy) using the standard relationship:

$$T\Delta S_b = \Delta H_b - \Delta G_b \quad (5)$$

These calculations enabled us to generate complete thermodynamic profiles for the binding of tobramycin to the p(rI)·p(rC) host duplex over a range of pH values. The resulting profiles are summarized in Table 5. Note that increasing pH results in a more favorable (negative) binding enthalpy (ΔH_b) and a less favorable (positive) entropic contribution to binding ($T\Delta S_b$). These pH-dependent changes in binding enthalpy and entropy are consistent with binding-induced protonation of one or more amino groups on the drug, since such protonation events are enthalpically favorable, while being entropically costly. In the pH range of 5.5 ⩽ pH ⩽ 6.5, the pH-induced decrease in binding entropy is completely offset by the corresponding increase in binding enthalpy, thereby yielding a similar binding free energy at 25 °C (ΔG_{b-25}) of approximately −10.5 kcal/mol. Thus, enthalpy-entropy compensations cause tobramycin to exhibit

Table 4. Electrostatic contributions to the complexation of tobramycin with the p(rI)·p(rC) duplex

pH	$-m\psi$[a]	m[a]	log(K°)[b]
5.5	−2.9 ± 0.1	3.2 ± 0.2	4.15 ± 0.17
7.0	−2.8 ± 0.1	3.1 ± 0.2	3.95 ± 0.25

[a] m denotes the number of ion pairs formed between tobramycin and the host RNA duplex. ψ denotes the thermodynamic counterion binding parameter, expressed as the fraction of a counterion bound per charge on the RNA polyanion (Record *et al.*, 1976). Values of m were determined from the slopes of the log(K_{25}) *versus* log([Na^+]) plots shown in Figure 5, using a ψ value of 0.89 for p(rI)·p(rC) (Record *et al.*, 1978).

[b] Values of log(K°) were derived from the y-intercepts of the log(K_{25}) *versus* log([Na^+]) plots shown in Figure 5.

Table 5. pH dependence of the thermodynamic parameters for the binding of tobramycin to the p(rI)·p(rC) duplex in the presence of 60 mM Na^+

pH	ΔH_b (kcal/mol)	[a] $T\Delta S_b$ (kcal/mol)	[b] ΔG_{b-25} (kcal/mol)	K_{25} (kcal/mol)
5.5	-2.2 ± 0.2	$+8.3 \pm 0.3$	-10.5 ± 0.1	$46(\pm 7) \times 10^6$
6.0	-4.7 ± 0.2	$+5.8 \pm 0.3$	-10.5 ± 0.1	$50(\pm 7) \times 10^6$
6.5	-6.8 ± 0.1	$+3.6 \pm 0.2$	-10.4 ± 0.1	$44(\pm 6) \times 10^6$
7.0	-8.2 ± 0.1	$+1.8 \pm 0.2$	-10.0 ± 0.1	$20(\pm 3) \times 10^6$
7.5	-10.5 ± 0.1	-1.0 ± 0.2	-9.5 ± 0.1	$8.9(\pm 1.3) \times 10^6$
8.0	-13.8 ± 0.1	-5.3 ± 0.2	-8.5 ± 0.1	$1.8(\pm 0.3) \times 10^6$

[a] ΔS_b is the binding entropy, as determined using equation (3) and the corresponding values of ΔH_b and ΔG_{b-25}.
[b] ΔG_{b-25} is the binding free energy at 25 °C, as determined using equation (2) and the corresponding value of K_{25}.

a similar affinity for p(rI)·p(rC) over the pH range of 5.5 to 6.5. Although the affinity of tobramycin for the p(rI)·p(rC) duplex is essentially constant over this pH range, the thermodynamic driving forces that dictate this affinity differ markedly with pH. At pH 5.5, tobramycin binding is primarily (79 %) entropy driven, while being primarily (65 %) enthalpy driven at pH 6.5. Recall that our salt-dependent binding data (Table 4) were consistent with tobramycin forming three ion pairs with the host RNA. Formation of these three ion pairs will result in the concomitant release of three Na^+ counterions from the host RNA. In addition to the release of Na^+ counterions, our acoustic and densimetric measurements (data to be published separately) were consistent with a tobramycin binding-induced release of both drug and RNA-bound water molecules as well. Thus, it is reasonable to suggest that the entropic driving force for tobramycin-p(rI)·p(rC) complexation at pH 5.5 is derived, at least in part, from the binding-induced release of Na^+ counterions, as well as the desolvation of both the drug and the host RNA.

In contrast to the compensating changes in ΔH_b and $T\Delta S_b$ that accompany pH changes within the 5.5-6.5 range, the corresponding changes in ΔH_b and $T\Delta S_b$ that accompany pH changes within the 6.5-8.0 range are not fully compensatory. Specifically, the loss in binding entropy associated with an increase in pH above a value of 6.5 is only partially compensated by the corresponding gain in binding enthalpy. Since the compensation is not complete, the net result is that increasing the pH above 6.5 decreases ΔG_{b-25}, with this reduction in binding affinity being entirely entropic in origin. In other words, raising the pH above a value of 6.5 lowers the affinity of the drug for the host RNA because the corresponding gain in enthalpy resulting from binding-induced protonation of the drug is not sufficient to compensate the concomitant loss in entropy.

Viscometric measurements are consistent with a tobramycin binding-induced reduction in the apparent molecular length of the host RNA duplex

The mode of binding by which a ligand interacts with a polymeric host nucleic acid duplex can be investigated by viscometric techniques (Bloomfield *et al.*, 1974). If one treats an RNA helix as a rod-like molecule and assumes negligible changes in the axial ratio upon ligand binding (Cohen & Eisenberg, 1969), the relationship between the relative solution viscosity (η/η_0) and the relative molecular length (L/L_0) is given by the following expression (Müller & Crothers, 1968; Bloomfield *et al.*, 1974):

$$\frac{L}{L_0} = \sqrt[3]{\frac{\eta}{\eta_0}} \qquad (6)$$

In this expression, L_0 denotes the apparent molecular length of the RNA in the absence of ligand and η_0 denotes the viscosity of the ligand-free RNA solution. Equation (6) postulates that a change in relative viscosity is reflected by a corresponding change in apparent molecular length. Ligand insertion between stacked base-pairs within a linear host duplex (intercalation) is associated with a lengthening of the nucleic acid molecule. This increase in nucleic acid length manifests itself as an increase in the viscosity of the nucleic acid solution. Thus, a ligand-induced increase in the viscosity of a nucleic acid solution is consistent with an intercalative mode of binding. Conversely, the lack of a ligand-induced increase in the viscosity of the nucleic acid solution is consistent with a non-intercalative mode of complexation (e.g. major or minor groove-directed binding).

Figure 6 shows the effects of tobramycin and ethidium bromide binding on the relative solution viscosity (η/η_0) of the p(rI)·p(rC) duplex at 60 mM Na^+ and pH 5.7. Note that addition of the classic intercalator ethidium bromide results in the expected viscosity profile for intercalation, namely, a drug-induced increase in RNA solution viscosity. By contrast, upon addition of tobramycin to an r_{bp} ratio of 0.21, the viscosity of the RNA solution decreases to an extent approximately 0.88-fold that of the drug-free duplex. This observation is consistent with tobramycin binding to the host p(rI)·p(rC) duplex non-intercalatively, in agreement with the major groove-directed mode of RNA binding observed by the Puglisi (Fourmy *et al.*, 1996, 1998a,b), Patel (Jiang *et al.*, 1997; Jiang & Patel, 1998), and Shafer (Chen *et al.*, 1997) groups in their NMR studies of aminoglycoside-RNA complexes.

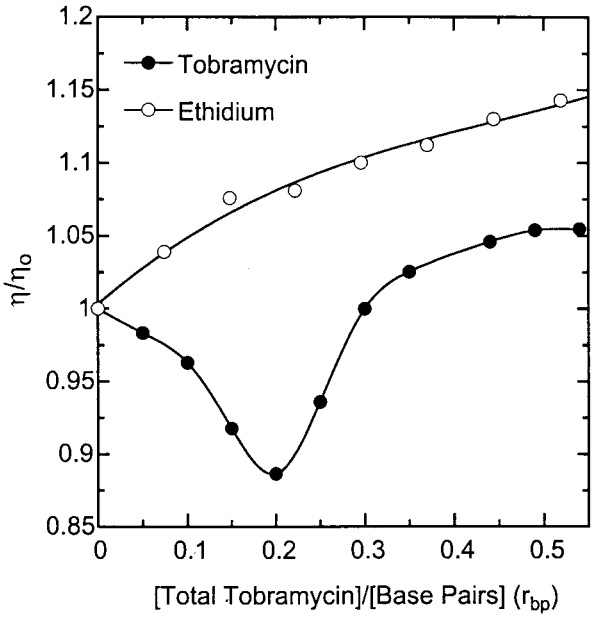

Figure 6. Viscometric titrations at 25.1 °C of p(rI)·p(rC) with ethidium bromide (open circles) or tobramycin (filled circles). η/η_0 is the relative solution viscosity and is defined in the text. All viscosity experiments were conducted at pH 5.7 in a buffer containing 10 mM sodium cacodylate (7 mM Na^+), 10 mM Mops (9.5 mM Na^+), 43.5 mM NaCl, and 0.1 mM EDTA.

In addition to suggesting a non-intercalative mode of RNA binding, the observed tobramycin-induced decrease in solution viscosity is consistent with a binding-induced, conformational change in the host RNA that reduces its effective molecular length. Such a conformational change could arise from a tobramycin binding-induced bend in the host RNA helix. In this connection, Puglisi and co-workers have shown that the major groove-directed binding of the aminoglycoside antibiotic paromomycin to an oligonucleotide modeling the *A*-site of the *E. coli* 16 S rRNA causes the host RNA to bend in the direction of the major groove (Fourmy *et al.*, 1998b). Another potential conformational change in the host RNA that can reduce its apparent molecular length is a change in a base-pair configurational parameter commonly termed ''slide'' (Calladine & Drew, 1992; Lu *et al.*, 1999). A sliding of the base-pairs relative to one another causes their displacement with respect to the helical axis, which, in turn, can result in a shortened helix with a narrower major groove and a widened minor groove. Note that both the bending of a helix and base-pair sliding are enthalpically unfavorable changes in nucleic acid structure, due to at least partial disruption of the stacking interactions between neighboring base-pairs. Thus, our observation that tobramycin-p(rI)·p(rC) complexation is only 21% enthalpy driven at pH 5.5 (i.e. in the absence of drug protonation effects) (see Table 5) may reflect an enthalpic penalty resulting from the induction of such alterations in RNA structure by tobramycin complexation.

Further inspection of Figure 6 reveals that addition of tobramycin beyond an r_{bp} ratio of 0.21 causes the viscosity of the RNA solution to increase to an extent that is approximately 1.05-fold that of the drug-free duplex. This increase in duplex solution viscosity may correspond to a secondary mode of tobramycin binding in which non-specific, electrostatically driven interactions between the cationic drug and the anionic phosphates of the RNA occur under conditions of high drug loading (high r_{bp} ratios). Such a binding mode may increase the stiffness and thus the solution viscosity of the host RNA helix.

Computer modeling studies suggest that tobramycin binds in the major groove of the p(rI)·p(rC) duplex, with the resulting complex being stabilized, at least in part, by the formation of specific hydrogen bonds

To gain insight into the potential structural nature of the tobramycin-p(rI)·p(rC) complex, we used the computer modeling methods described in Materials and Methods to explore the energetically feasible structures that this complex might adopt. Figure 7 shows a stereo view (looking into the RNA major groove) of a low-energy structure that emerged from these studies. In this model, the drug is in its fully protonated, pentacationic state. Note that the drug sits deep in the floor of the major groove and covers approximately four base-pairs, an observation consistent with our CD-derived binding site size discussed above (see Figure 2). Repeated attempts to dock the tobramycin molecule into the minor groove of the host RNA duplex failed to yield a stable low-energy structure. This observation suggests that the minor groove of *A*-form double-helical RNA is not a good binding site for aminoglycosides, and, as such, is consistent with previously reported NMR studies (Fourmy *et al.*, 1996, 1998a; Chen *et al.*, 1997; Jiang *et al.*, 1997; Jiang & Patel, 1998), which revealed the major groove to be the preferred site of aminoglycoside interaction. Further inspection of the model in Figure 7 reveals that each of the drug saccharide rings forms two hydrogen bonds (denoted by the blue broken lines) with the host RNA. Specifically, the 2′-hydroxyl moiety of ring III forms hydrogen bonds with the O6 atoms of neighboring inosine residues, while the 1-amino group of ring I forms hydrogen bonds with the O6 and N7 atoms of neighboring inosines. In contrast to the hydrogen bond-forming moieties of rings I and III, the 2′- and 6′-amino groups of ring II form hydrogen bonds with oxygen atoms on the phosphate backbone of the p(rC) strand, rather than with base atoms on the p(rI) strand. In the aggregate, these observations suggest that the formation of specific hydrogen bonds between accepting groups on the drug and donating groups on both the bases and the phosphate backbone of the host

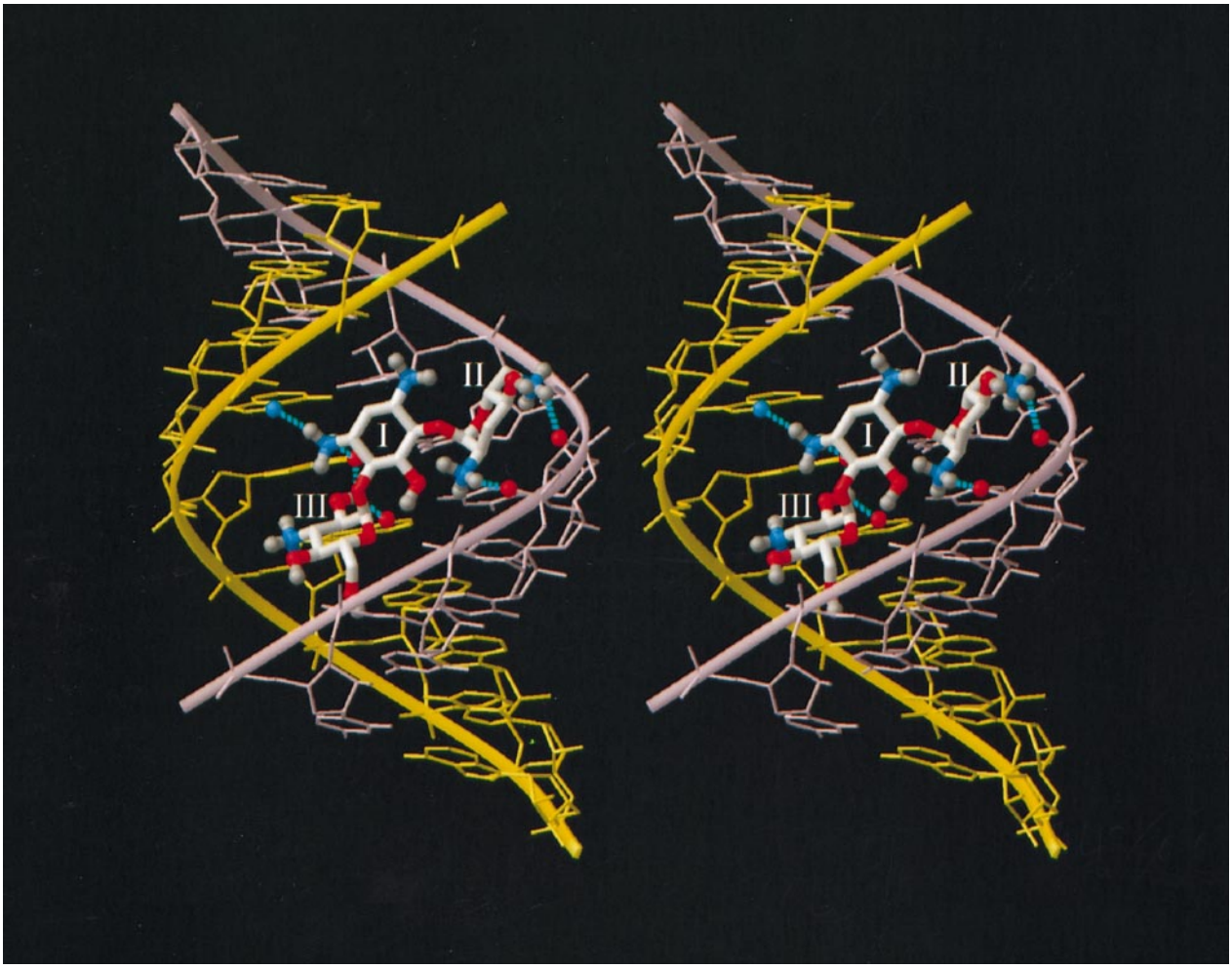

Figure 7. Stereo view (looking into the RNA major groove) of a model for the complex formed between p(rI)·p(rC) and the fully protonated, pentacationic form of tobramycin. The p(rI) strand is in gold, while the p(rC) strand is in purple. Tobramycin is depicted according to the following color convention: carbon, white; oxygen, red; nitrogen, blue; hydrogen, gray. The ring numbers of the drug are indicated in Roman numerals. Potential hydrogen bonding contacts between the drug and the host RNA are depicted as blue broken lines.

RNA contributes, at least in part, to the stability of the tobramycin-p(rI)·p(rC) complex. In fact, such drug-RNA hydrogen bonding interactions may account for that portion (2.2 out of 10.5 kcal/mol, or 21%) of the total free energy associated with tobramycin-p(rI)·p(rC) complexation in the absence of drug protonation effects (i.e. at pH 5.5) that is enthalpic in origin (see Table 5).

Recall that our pH-dependent binding data discussed above (Tables 1 and 2) were consistent with the binding-induced protonation of one or more drug amino groups at pH values greater than 5.5. The structural model shown in Figure 7 suggests that at least one of the relevant amino group(s) may be located at the 2′, 6′, and/or 1-positions, since they form specific hydrogen bonds with the host RNA. Note that the amino groups at positions 1 and 2′ have substantially lower pK_a values (p$K_{a-1} = 7.4$ and p$K_{a-2'} = 7.6$) than the amino group at the 6′ position (p$K_{a-6'} = 8.6$) (see Figure 1). Hence, these two amino groups are particularly good candidates for being sites at which binding-induced protonation might occur.

Concluding Remarks

We have used a combination of spectroscopic and calorimetric techniques to demonstrate that the binding of the aminoglycoside antibiotic tobramycin to an *A*-form RNA duplex is sensitive to both the pH and Na^+ concentration. These salt and pH dependencies are consistent with tobramycin binding to the host RNA as a trication (i.e. forming three ion pairs with the host RNA), as well as with binding-induced protonation of one or more drug amino groups at pH values where the drug is not fully protonated. In addition, we have shown that the binding of tobramycin to the host RNA duplex is entropy driven at pH values $\leqslant 6.0$, while being enthalpy driven at pH values >6.0. To the best of

our knowledge, these studies represent the first quantitative thermodynamic investigation of aminoglycoside-RNA recognition. We also have shown that tobramycin binding to the host RNA duplex induces a change in its viscometric properties consistent with a drug-induced reduction in its apparent molecular length. We have used computer modeling techniques to derive a structural model of the tobramycin-RNA complex which revealed the formation of specific hydrogen bonds between acceptor groups on the drug and donor groups in the major groove of the host RNA. Taken together, these observations suggest that tobramycin-RNA complexation is governed by a broad range of factors, including solution conditions, electrostatic interactions, hydrogen bonding interactions, drug protonation reactions, and binding-induced structural alterations in the host RNA.

Generally, the results reported here have intrinsic value, in that they contribute to the broad-based effort to define the molecular recognition patterns that control the affinities and specificities of RNA-binding ligands. Such knowledge is required for the ultimate development of a more rational approach to drug design. Our results also may have a more practical impact based on the observations by several groups that RNA regions containing loops and/or bulges often serve as high affinity sites for aminoglycoside recognition (reviewed by Wallis & Schroeder, 1997; Michael & Tor, 1998; Tor, 1999; Schroeder *et al*., 2000). In this connection, Puglisi and co-workers have shown that the aminoglycoside antibiotic, paromomycin, preferentially binds to an asymmetric loop region of an oligonucleotide that models the *A*-site of the *E. coli* 16 S rRNA (Fourmy *et al*., 1996, 1998a,b). Significantly, they note that the major groove-directed binding of paromomycin induces a conformational change in the host RNA, one feature of which is a drug-induced bending of the RNA helix in the direction of the major groove (Fourmy *et al*., 1998b). Recall that our viscometric data were consistent with a tobramycin-induced reduction in the apparent molecular length of the p(rI)·p(rC) duplex. Such a structural alteration could arise from a binding-induced bend in the host RNA helix. Note that the bending of a nucleic acid double helix is an energetically unfavorable process, due, in large part, to the disruption of stacking interactions between neighboring base-pairs (Park & Breslauer, 1991; Poklar *et al*., 1996). Regions of duplex RNA that contain loops or bulges may serve to minimize this energetic penalty, thereby enhancing their aminoglycoside binding affinities relative to those exhibited by duplex RNA regions that lack such structures. In other words, loop-containing regions of duplex RNA may be energetically predisposed toward the types of altered (e.g. bent) conformations favored by aminoglycosides. Clearly, other factors, such as specific hydrogen bonding interactions between the drug and the host RNA, also contribute to the observed specificities with which aminoglycosides bind RNA, since not all looped regions of RNA are targeted preferentially by aminoglycosides. Several such interactions were revealed by the NMR studies noted above on the paromomycin-rRNA complex (Fourmy *et al*., 1996, 1998a,b). The thermodynamic and hydrodynamic results presented here provide one potential explanation for the structure-specific RNA binding behavior exhibited by aminoglycosides that serve as a basis for further discussion.

Materials and Methods

RNA and drug molecules

The polynucleotide, p(rI)·p(rC), was obtained from Pharmacia Biotech, Inc. (Piscataway, NJ) and was used without further purification. The concentrations of all p(rI)·p(rC) solutions were determined spectrophotometrically using an extinction coefficient at 260 nm (ε_{260}) of 5150 (mol nucleotide/l)$^{-1}$ cm^{-1} (Chamberlin, 1965). The free base of tobramycin was obtained from Fluka (Milwaukee, WI) and was used without further purification. Stock solutions of tobramycin (at concentrations of 10 to 15 mM) were prepared in distilled water.

UV spectrophotometry

All UV absorbance experiments were conducted on an AVIV Model 14DS Spectrophotometer (Aviv Associates; Lakewood, NJ) equipped with a thermoelectrically controlled cell holder. A quartz cell with a 1 cm pathlength was used for all the absorbance studies. Absorbance *versus* temperature profiles were measured at 246 nm with a five seconds averaging time. The temperature was raised in 0.5 deg. C increments, and the samples were allowed to equilibrate for one minute at each temperature setting. In these thermal denaturation studies, the p(rI)·p(rC) solutions were 40 μM in base-pair and contained either 0 or 10 μM tobramycin. The buffer solutions for the UV melting experiments contained 10 mM sodium cacodylate (7 mM Na^+), 10 mM Mops (9.5 mM Na^+), 0.1 mM EDTA, and NaCl at concentrations ranging from 18.5 to 333.5 mM. The pH values of the experimental buffer solutions ranged from 5.5 to 8.0, and were adjusted, when necessary, by addition of 1 N HCl. For each optically detected transition, the melting temperature (T_m) was determined as described (Marky & Breslauer, 1987).

CD spectropolarimetry

All CD experiments were conducted at 25 °C on an AVIV Model 60DS Spectropolarimeter (Aviv Associates; Lakewood, NJ) equipped with a thermoelectrically controlled cell holder. A quartz cell with a 1 cm pathlength was used in the CD studies. CD spectra were recorded from 220 to 320 nm in 1 nm increments with an averaging time of two seconds. The tobramycin titration was performed by incrementally adding 1.5-4 μl aliquots of 1 mM tobramycin into a p(rI)·p(rC) solution (1 ml) that was 60 μM in base-pair. The buffer conditions for the tobramycin titration were 10 mM sodium cacodylate (7 mM Na^+), 10 mM Mops (9.5 mM Na^+), 43.5 mM NaCl, 0.1 mM EDTA, and pH 6.0. The final CD spectra

for the titration were normalized to reflect equimolar RNA concentrations.

Isothermal titration calorimetry (ITC)

Isothermal calorimetric measurements were performed at 25 °C on a MicroCal MCS Titration Calorimeter (MicroCal, Inc., Northampton, MA). In a typical experiment, 5 μl aliquots of 2 mM tobramycin were injected from a 250 μl rotating syringe into an isothermal sample chamber containing 1.31 ml of a p(rI)·p(rC) solution that was 500 μM base-pair. Each experiment of this type was accompanied by the corresponding control experiment in which 5 μl aliquots of 2 mM tobramycin were injected into a solution of buffer alone. The duration of each injection was 6.3 seconds and the delay between injections was 300 seconds. The initial delay prior to the first injection was 60 seconds. Each injection generated a heat burst curve (μcal/second *versus* seconds). The area under each curve was determined by integration (using the Origin version 4.1 software (MicroCal, Inc., Northampton, MA)) to obtain a measure of the heat associated with that injection. The heat associated with each tobramycin-buffer injection was subtracted from the corresponding heat associated with each tobramycin-p(rI)·p(rC) injection to yield the heat of tobramycin binding for that injection. The calorimeter was calibrated both electronically and chemically as described (Pilch *et al*., 1995a,b). The buffer solutions for the ITC experiments contained 10 mM sodium cacodylate (7 mM Na^+), 10 mM Mops (9.5 mM Na^+), 43.5 mM NaCl, and 0.1 mM EDTA. The pH values of the ITC experimental solutions ranged from 5.5 to 8.0.

Differential scanning calorimetry (DSC)

Heat capacity (ΔCp) *versus* temperature (T) profiles for the thermally induced transitions of the drug-free p(rI)·p(rC) duplex were measured at pH values ranging from 5.5 to 8.0 using a Model 5100 Nano Differential Scanning Calorimeter (Calorimetry Science Corp., Provo, UT). The heating rate was 1 deg. C/minute. The Watson-Crick transition enthalpy (ΔH_{WC}) was calculated from the area under each heat capacity curve using the Origin version 4.1 software (MicroCal, Inc., Northampton, MA). The RNA duplex solutions were 200 μM in base-pair.

Viscometry

Viscosity measurements were conducted in a Cannon-Manning size 75 capillary viscometer (Thomas Scientific; Swedesboro, NJ) that was submerged in a water bath maintained at 25.1 (±0.1)°C. Flow times were measured two to five times to an accuracy of ±0.3 seconds with a stopwatch, and the average time over all replicates was recorded. Viscosity studies on p(rI)·p(rC) were conducted at pH 5.7 in buffer containing 10 mM sodium cacodylate (7 mM Na^+), 10 mM Mops (9.5 mM Na^+), 43.5 mM NaCl, and 0.1 mM EDTA. Aliquots (4-6 μl) of either 6.2 mM ethidium bromide (EtBr) or 6.2 mM tobramycin were titrated directly into the viscometer containing a p(rI)·p(rC) solution (1 ml) that was 500 μM in base-pair, and flow times in the range of 155 to 167 seconds were measured after each addition.

Computer modeling

An automated *ab initio* drug-RNA docking procedure was implemented with the ICM molecular modeling software by Molsoft (Abagyan *et al*., 1994; Totrov & Abagyan, 1997). Structural coordinates for the p(rI)·p(rC) duplex were derived from the X-ray fiber diffraction data reported by Arnott *et al*. (1973), while the atomic coordinates of tobramycin were derived from the NMR structure of a tobramycin-RNA aptamer complex reported recently by the Patel group (Jiang *et al*., 1997; Jiang & Patel, 1998). The RNA docking procedure involved three steps. In the first step, both the RNA and the drug were treated as rigid bodies, with only the six spatial coordinates of the drug being allowed to vary. The RNA was modeled using precalculated, three-dimensional grid potential maps (with a grid size of 0.5 Å). These grid potentials incorporate van der Waals, electrostatic, and hydrogen bonding energy terms (Totrov & Abagyan, 1997). Using randomized starting positions for the drug, 100 independent Monte Carlo minimizations of 10,000 steps each were conducted. In the second step, the ten lowest energy conformations of the drug-RNA complex obtained from the Monte Carlo minimizations were superimposed, and their structures were compared. This comparison yielded four distinct groups of conformations. One representative conformation from each group was selected for further minimization. In the third step, the structure of the drug-RNA complex was refined further using the Amber force field (Weiner *et al*., 1986; Veal & Wilson, 1991) rather than grid potentials. In these calculations, the torsion angles of both the drug and the RNA were allowed to vary. As a result of this final refinement, the structures of both the drug and the RNA were altered slightly relative to their starting conformations (the root-mean-square deviation was less than 0.5 Å for tobramycin and less than 1.1 Å for the RNA duplex). One manifestation of the binding-induced alteration in the structure of the host RNA duplex was a 1.5 Å reduction in the width of the major groove.

Acknowledgments

The authors thank Mr Carl Pavel for his participation in the preliminary studies that led to this investigation, Dr A. R. Srinivasan for his assistance in the preparation of the computer modeling figure, and Dr Kenneth J. Breslauer for many helpful discussions. This work was supported by grants from the American Cancer Society (RPG-99-153-01-CDD) to (D.S.P.), the National Institutes of Health (CA77433 (D.S.P.) and GM20861 (W.K.O.)), and the New Jersey Commission on Cancer Research (00-64-CCR-S-0) to (D.S.P.)). V.K. was supported by a postdoctoral fellowship from the Program in Mathematics and Molecular Biology based at Florida State University.

References

Abagyan, R., Totrov, M. & Kuznetsov, D. (1994). ICM - A new method for protein modeling and design - applications to docking and structure prediction from the distorted native conformation. *J. Comput. Chem.* **15**, 488-506.

Arnott, S., Hukins, D. W. L., Dover, S. D., Fuller, W. & Hodgson, A. R. (1973). Structures of synthetic poly-

nucleotides in the A-RNA and A′-RNA conformations: X-ray diffraction analyses of the molecular conformations of polyadenylic acid·polyuridylic acid and polyinosinic acid·polycytidylic acid. *J. Mol. Biol.* **81**, 107-122.

Bloomfield, V. A., Crothers, D. M. & Tinoco, I., Jr (1974). *Physical Chemistry of Nucleic Acids*, Harper & Row, New York.

Bruhn, S. L., Toney, J. L. & Lippard, S. J. (1990). Biological processing of DNA modified by platinum compounds. *Prog. Inorg. Chem.* **38**, 477-516.

Calladine, C. R. & Drew, H. R. (1992). *Understanding DNA: The Molecule & How It Works*, Academic Press, San Diego.

Chamberlin, M. J. (1965). Comparative properties of DNA, RNA, and hybrid homopolymer pairs. *Fed. Proc.* **24**, 1446-1457.

Chambers, H. F. & Sande, M. A. (1996). The aminoglycosides. In *Goodman & Gilman's The Pharmacological Basis of Therapeutics* (Hardman, J. G., Limbird, L. E., Molinoff, P. B., Ruddon, R. W. & Gilman, Goodman A., eds), 9th edit., pp. 1103-1121, McGraw-Hill, New York.

Chen, Q., Shafer, R. H. & Kuntz, I. D. (1997). Structure-based discovery of ligands targeted to the RNA double helix. *Biochemistry,* **36**, 11402-11407.

Chow, C. S. & Bogdan, F. M. (1997). A structural basis for RNA-ligand interactions. *Chem. Rev.* **97**, 1489-1513.

Clouet-d'Orval, B., Stage, T. K. & Uhlenbeck, O. C. (1995). Neomycin inhibition of the hammerhead rybozyme involves ionic interactions. *Biochemistry,* **34**, 11186-11190.

Cohen, G. & Eisenberg, H. (1969). Viscosity and sedimentation study of sonicated DNA-proflavine complexes. *Biopolymers,* **8**, 45-55.

Crothers, D. M. (1971). Statistical thermodynamics of nucleic acid melting transitions with coupled binding equilibria. *Biopolymers,* **10**, 2147-2160.

deHaseth, P. L., Lohman, T. M. & Record, M. T. J. (1977). Non-specific interaction of *lac* repressor with DNA: an association reaction driven by counterion release. *Biochemistry,* **16**, 4783-4790.

Dorman, D. E., Paschal, J. W. & Merkel, K. E. (1976). ^{15}N nuclear magnetic resonance spectroscopy. The nebramycin aminoglycosides. *J. Am. Chem. Soc.* **98**, 6885-6888.

Douthart, R. J., Burnett, J. P., Beasley, F. W. & Frank, B. H. (1973). Binding of ethidium bromide to double-stranded ribonucleic acid. *Biochemistry,* **12**, 214-220.

Ecker, D. J. & Griffey, R. H. (1999). RNA as a small-molecule drug target: doubling the value of genomics. *Drug Discov. Today,* **4**, 420-429.

Fourmy, D., Recht, M. I., Blanchard, S. C. & Puglisi, J. D. (1996). Structure of the *A*-site of *Escherichia coli* 16 S ribosomal RNA complexed with an aminoglycoside antibiotic. *Science,* **274**, 1367-1371.

Fourmy, D., Recht, M. I. & Puglisi, J. D. (1998a). Binding of neomycin-class aminoglycoside antibiotics to the *A*-site of 16 S rRNA. *J. Mol. Biol.* **277**, 347-362.

Fourmy, D., Yoshizawa, S. & Puglisi, J. D. (1998b). Paromomycin binding induces a local conformational change in the *A*-site of 16 S rRNA. *J. Mol. Biol.* **277**, 333-345.

Gelasco, A. & Lippard, S. J. (1998). NMR solution structure of a DNA dodecamer duplex containing a *cis*-diammineplatinum(II) d(GpG) intrastrand cross-link, the major adduct of the anticancer drug cisplatin. *Biochemistry,* **37**, 9230-9239.

Hamasaki, K., Killian, J., Cho, J. & Rando, R. R. (1998). Minimal RNA constructs that specifically bind aminoglycoside antibiotics with high affinities. *Biochemistry,* **37**, 656-663.

Hamy, F., Brondani, V., Flörsheimer, A., Stark, W., Blommers, M. J. J. & Klimkait, T. (1998). A new class of HIV-1 tat antagonist acting through tat-TAR inhibition. *Biochemistry,* **37**, 5086-5095.

Hendrix, M., Priestly, E. S., Joyce, G. F. & Wong, C. (1997). Direct observation of aminoglycoside-RNA interactions by surface plasmon resonance. *J. Am. Chem. Soc.* **119**, 3641-3648.

Hermann, D. & Guschlbauer, W. (1978). Interaction of Pt (II) compounds with a synthetic polyribonucleotide complex, Poly(I)·Poly(C). *Biochimie,* **60**, 1046-1048.

Hermann, T. & Westhof, E. (1998). Aminoglycoside binding to the hammerhead ribozyme: a general model for the interaction of cationic antibiotics with RNA. *J. Mol. Biol.* **276**, 903-912.

Jiang, L. & Patel, D. J. (1998). Solution structure of the tobramycin-RNA aptamer complex. *Nature Struct. Biol.* **5**, 769-774.

Jiang, L., Suri, A. K., Fiala, R. & Patel, D. J. (1997). Saccharide-RNA recognition in an aminoglycoside antibiotic-RNA aptamer complex. *Chem. Biol.* **4**, 35-50.

Kirk, S. R. & Tor, Y. (1999). tRNA(Phe) binds aminoglycoside antibiotics. *Bioorg. Med. Chem.* **7**, 1979-1991.

Koch, K. F., Merkel, K. E., O'Connor, S. C., Occolowitz, J. L., Paschal, J. W. & Dorman, D. E. (1978). Structures of some of the minor aminoglycoside factors of the nebramycin fermentation. *J. Org. Chem.* **43**, 1430-1434.

Lato, S. M., Boles, A. R. & Ellington, A. D. (1995). *In Vitro* selection of RNA lectins: using combinatorial chemistry to interpret ribozyme evolution. *Chem. Biol.* **2**, 291-303.

Liu, Y., Tidwell, R. R. & Leibowitz, M. J. (1994). Inhibition of *in vitro* splicing of a group I intron of *Pneumocystis carinii*. *J. Euk. Microbiol.* **41**, 31-38.

Lu, X.-J., Babcock, M. S. & Olson, W. K. (1999). Overview of nucleic acid analysis programs. *J. Biomol. Struct. Dynam.* **16**, 833-843.

Marky, L. A. & Breslauer, K. J. (1987). Calculating thermodynamic data for transitions of any molecularity from equilibrium melting curves. *Biopolymers,* **26**, 1601-1620.

McGhee, J. D. (1976). Theoretical calculations of the helix-coil transition of DNA in the presence of large, cooperatively binding ligands. *Biopolymers,* **15**, 1345-1375.

Mei, H.-Y., Cui, M., Heldsinger, A., Lemrow, S. M., Loo, J. A., Sannes-Lowry, K. A., Sharmeen, L. & Czarnik, A. W. (1998). Inhibitors of protein-RNA complexation that target the RNA: specific recognition of human immunodeficiency virus type I TAR RNA by small organic molecules. *Biochemistry,* **37**, 14204-14212.

Michael, K. & Tor, Y. (1998). Designing novel RNA binders. *Chem. Eur. J.* **4**, 2091-2098.

Miyamoto, S. & Kazuko, M. (1958). Dissociation constant and heat of ionization of D-glucosamine. *Kyoritsu Yakka Daigaku Kenkyû Nempô,* **4**, 12-16.

Müller, W. & Crothers, D. M. (1968). Studies of the binding of actinomycin and related compounds to DNA. *J. Mol. Biol.* **35**, 251-290.

Nelson, J. W. & Tinoco, I., Jr (1984). Intercalation of ethidium ion into RNA and DNA oligonucleotides. *Biopolymers,* **23**, 213-233.

Park, Y.-W. & Breslauer, K. J. (1991). A spectroscopic and calorimetric study of the melting behaviors of a ''bent'' and a ''normal'' DNA duplex: $(d(GA_4T_4C))_2$ *versus* $(d(GT_4A_4C))_2$. *Proc. Natl Acad. Sci. USA,* **88**, 1551-1555.

Patel, D. J., Suri, A. K., Jiang, F., Jiang, L., Fan, P., Kumar, R. A. & Nonin, S. (1997). Structure, recognition and adaptive binding in RNA aptamer complexes. *J. Mol. Biol.* **272**, 645-664.

Pilch, D. S., Kirolos, M. A. & Breslauer, K. J. (1995a). Berenil binding to higher ordered nucleic acid structures: complexation with a DNA and RNA triple helix. *Biochemistry,* **34**, 16107-16124.

Pilch, D. S., Kirolos, M. A., Liu, X., Plum, G. E. & Breslauer, K. J. (1995b). Berenil (1,3-bis-(4′-amidinophenyl)triazene) Binding to DNA duplexes and to a RNA duplex: evidence for both intercalative and minor groove binding properties. *Biochemistry,* **34**, 9962-9976.

Poklar, N., Pilch, D. S., Lippard, S. J., Redding, E. A., Dunham, S. U. & Breslauer, K. J. (1996). Influence of cisplatin intrastrand crosslinking on the conformation, thermal stability, and energetics of a 20-mer DNA duplex. *Proc. Natl Acad. Sci. USA,* **93**, 7606-7611.

Recht, M. I., Fourmy, D., Blanchard, S. C., Dahlquist, K. D. & Puglisi, J. D. (1996). RNA sequence determinants for aminoglycoside binding to an *A*-site rRNA model oligonucleotide. *J. Mol. Biol.* **262**, 421-436.

Record, M. T. J., Lohman, T. M. & de Haseth, P. (1976). Ion effects on ligand-nucleic acid interactions. *J. Mol. Biol.* **107**, 145-158.

Record, M. T. J., Anderson, C. F. & Lohman, T. M. (1978). Thermodynamic analysis of ion effects on the binding and conformational equilibria of proteins and nucleic acids: the roles of ion association or release, screening, and ion effects on water activity. *Quart. Rev. Biophys.* **11**, 103-178.

Robinson, H. & Wang, A. H.-J. (1996). Neomycin, spermine and hexaamminecobalt(III) share common structural motifs in converting *B* to *A*-DNA. *Nucl. Acids Res.* **24**, 676-682.

Ryan, P. C. & Draper, D. E. (1991). Detection of a key tertiary interaction in the highly conserved GTPase center of large subunit ribosomal RNA. *Proc. Natl Acad. Sci. USA,* **88**, 6308-6312.

Saenger, W. (1983). *Principles of Nucleic Acid Structure*, Springer-Verlag, New York.

Schroeder, R. & von Ahsen, U. (1996). Interaction of aminoglycoside antibiotics with RNA. In *Nucleic Acids and Molecular Biology* (Eckstein, F. & Lilley, D. M. J., eds), vol. 10, pp. 53-74, Springer-Verlag, Heidelberg.

Schroeder, R., Waldsich, C. & Wank, H. (2000). Modulation of RNA function by aminoglycoside antibiotics. *EMBO J.* **19**, 1-9.

Sherman, S. E. & Lippard, S. J. (1987). Structural aspects of platinum anticancer drug interactions with DNA. *Chem. Rev.* **87**, 1153-1181.

Spahn, C. M. & Prescott, C. D. (1996). Throwing a spanner in the works: antibiotics and the translation apparatus. *J. Mol. Med.* **74**, 423-439.

Stage, T. K., Hertel, K. J. & Uhlenbeck, O. C. (1995). Inhibition of the hammerhead ribozyme by neomycin. *RNA,* **1**, 95-101.

Takahara, P. M., Rosenzweig, A. C., Frederick, C. A. & Lippard, S. J. (1995). Crystal structure of double-stranded DNA containing the major adduct of the anticancer drug cisplatin. *Nature,* **377**, 649-652.

Takahara, P. M., Frederick, C. A. & Lippard, S. J. (1996). Crystal structure of the anticancer drug cisplatin bound to duplex DNA. *J. Am. Chem. Soc.* **118**, 12309-12321.

Tinoco, I., Jr, Sauer, K. & Wang, J. C. (1978). *Physical Chemistry: Principles and Applications in Biological Sciences*, Prentice-Hall, Englewood Cliffs.

Tor, Y. (1999). RNA and the small molecule world. *Angew. Chem. Int. Ed. Engl.* **38**, 1579-1582.

Totrov, M. & Abagyan, R. (1997). Flexible protein-ligand docking by global energy optimization in internal coordinates. *Proteins: Struct. Funct. Genet.* **1**, 215-220.

Vázquez, D. (1979). *Inhibitors of Protein Biosynthesis*, Springer-Verlag, New York.

Veal, J. M. & Wilson, W. D. (1991). Modeling of nucleic acid complexes with cationic ligands: a specialized molecular mechanics force field and its application. *J. Biomol. Struct. Dynam.* **8**, 1119-1145.

von Ahsen, U. & Noller, H. F. (1993). Footprinting the sites of interaction of antibiotics with catalytic group I intron RNA. *Science,* **260**, 1500-1503.

von Ahsen, U., Davies, J. & Schroeder, R. (1991). Antibiotic inhibition of group I ribozyme function. *Nature,* **353**, 368-370.

Waldsich, C., Semrad, K. & Schroeder, R. (1998). Neomycin B inhibits splicing of the *td* intron indirectly by interfering with translation and enhances misplicing *in vivo*. *RNA,* **4**, 1653-1663.

Wallis, M. G. & Schroeder, R. (1997). The binding of antibiotics to RNA. *Prog. Biophys. Mol. Biol.* **67**, 141-154.

Wallis, M. G., von Ahsen, U., Schroeder, R. & Famulok, M. (1995). A novel RNA motif for neomycin recognition. *Chem. Biol.* **2**, 543-552.

Wallis, M. G., Streicher, B., Wank, H., von Ahsen, U., Clodi, E., Wallace, S. T., Famulok, M. & Schroeder, R. (1997). *In vitro* selection of a viomycin-binding RNA pseudoknot. *Chem. Biol.* **4**, 357-366.

Wang, H. & Tor, Y. (1997). Electrostatic interactions in RNA aminoglycosides binding. *J. Am. Chem. Soc.* **119**, 8734-8735.

Wang, H. & Tor, Y. (1998). RNA-aminoglycoside interactions: design, synthesis, and binding of ''amino-aminoglycosides'' to RNA. *Angew. Chem. Int. Ed. Engl.* **37**, 109-111.

Wang, S., Huber, P. W., Cui, M., Czarnik, A. W. & Mei, H.-Y. (1998). Binding of neomycin to the TAR element of HIV-1 RNA induces dissociation of the Tat protein by an allosteric mechanism. *Biochemistry,* **37**, 5549-5557.

Wang, Y. & Rando, R. R. (1995). Specific binding of aminoglycoside antibiotics to RNA. *Chem. Biol.* **2**, 281-290.

Wang, Y., Killian, J., Hamasaki, K. & Rando, R. R. (1996). RNA molecules that specifically and stoichiometrically bind aminoglycoside antibiotics with high affinities. *Biochemistry,* **35**, 12328-12346.

Waring, M. J. (1966). Structural requirements for the binding of ethidium to nucleic acids. *Biochim. Biophys. Acta,* **114**, 234-244.

Weiner, S. J., Kollman, P. A., Nguyen, D. T. & Case, D. A. (1986). An all atom force field for simulation of proteins and nucleic acids. *J. Comput. Chem.* **7**, 230-252.

Werstuck, G. & Green, M. R. (1998). Controlling gene expression in living cells through small molecule-RNA interactions. *Science,* **282**, 296-298.

Werstuck, G., Zapp, M. L. & Green, M. L. (1996). A non-canonical base pair within the human immunodeficiency virus rev-responsive element is involved in both rev and small molecule recognition. *Chem. Biol.* **3**, 129-137.

Zapp, M. L., Stern, S. & Green, M. R. (1993). Small molecules that selectively block RNA binding of HIV-1 Rev protein inhibit Rev function and viral production. *Cell,* **74**, 969-978.

Zapp, M. L., Young, D. W., Kumar, A., Singh, R., Boykin, D. W., Wilson, W. D. & Green, M. R. (1997). Modulation of the Rev-RRE interactions by aromatic heterocyclic compounds. *Bioorg. Med. Chem.* **5**, 1149-1155.

Edited by I. Tinoco

(Received 28 December 1999; received in revised form 21 February 2000; accepted 21 February 2000)